

Cotton incorporated Poly(lactic acid)/thermoplastic Starch Based Composites Used as Flexible Packing for Short Shelf Life Products

Luciano Figueiredo Silva^a, Pedro Henrique Poubel Mendonça da Silveira^{a,b} ,
Ana Carolina Bastos Rodrigues^a, Sergio Neves Monteiro^b, Shirleny Fontes Santos^a ,
João Paulo Saraiva Morais^c, Daniele Cruz Bastos^{a*} 

^aUniversidade do Estado do Rio de Janeiro (UERJ), Avenida Manuel Caldeira de Alvarenga, 1203, Campo Grande, 23070-200, Rio de Janeiro, RJ, Brasil.

^bInstituto Militar de Engenharia (IME), Praça General Tibúrcio, 80, Urca, 22290-270, Rio de Janeiro, RJ, Brasil.

^cEmbrapa Algodão, Rua Oswaldo Cruz, 1143, Centenário, 58428095, Campina Grande, PB, Brasil.

Received: August 16, 2023; Revised: December 18, 2023; Accepted: February 14, 2024

Biocomposites have gained attention in the packaging industry due to their potential as sustainable alternatives to conventional synthetic materials. In this study, novel cotton incorporated poly (lactic acid)/thermoplastic starch biocomposites were developed for packaging applications using in short shelf life products the extrusion method. Pelletized samples obtained by extrusion were stamped from plates obtained by compression and were characterized through measurement of density, hardness, contact angle and water absorption, as well as Fourier transform infrared spectroscopy (FTIR), thermal analysis and scanning electron microscopy (SEM). No significant changes in the density results were observed. A slight increase in the hardness of formulations in relation to the PLA was associated with the presence of cotton fiber in biocomposites. The FTIR results revealed physical interaction of PLA, TPS and cotton fiber. By DSC analysis, for all formulations the melting exhibited only one peak, suggesting good homogeneity and interaction among the components, as observed by TG/DTG results, and corroborating SEM analysis. The biocomposite PLA/TPS/Cotton 85/10/5 wt.% displayed greater increase in water absorption than both 95/5/0 and 90/5/5 wt.% formulations, which can be attributed to the increase in starch proportion, confirming the contact angle results. The hydrophilic tendency corroborated the biodegradation process in the packaging end-of-life.

Keywords: PLA, TPS, Water Absorption, Thermal Properties, Mechanical Properties.

1. Introduction

The use of traditional plastic-based packaging has resulted in a huge amount of municipal solid waste, raising environmental concerns. It has been estimated that the quantities of municipal solid waste may markedly increase to 2200 million tonnes per year by 2025 because of the rapid urbanization progress and economic growth¹. Plastic packaging materials are made of numerous types of synthetic polymers, such as polyethylene (PE), polypropylene (PP) and polystyrene (PS), each containing plasticizing additives, which can assist in the processing of these plastics, and petrochemical-derived colorants that provide color or transparency to the material with the aim of influencing the material's design or application. Additionally, plastic packaging can be coated or composed of multiple layers of different polymers to enhance their thermal, mechanical and barrier properties, through parameter adjustment such as control of composition, pore size, thickness, polarity, swelling capacity, and solubility². The challenges associated

with collecting, identifying, sorting, transporting, cleaning, and reprocessing plastic packaging materials often make recycling economically impractical, thus making landfill disposal a more common alternative^{3,4}.

Recent technological advancements have led to the development of bio-based packaging materials made from biomass polymers such as starch, cellulose, lignin and chitin, such as biocomposites using natural fibers⁵⁻⁹. These compostable materials possess similar functionality to petroleum-based synthetic polymers, such as their structural integrity, flexibility, and versatility in various applications, but offer the added benefits of being inherently biodegradable. The shift from a linear economy to a circular economy can provide a new foundation for the market and utilization of plastic packaging, which will help to reduce environmental pollution^{3,4,10,11}. In light of this, eco-friendly and biodegradable materials such as polysaccharides, lipids and protein based biopolymers are being increasingly utilized for the preparation of biodegradable films, drug delivery and packaging materials¹²⁻¹⁵.

*e-mail: daniele.bastos@uerj.br

Poly(Lactic Acid) (PLA) is a biodegradable polymer derived from corn, cassava, sugar beet or sugarcane¹⁶. This aliphatic polyester has remarkable mechanical and chemical barrier properties, as well as biocompatibility and odorlessness, making it suitable for use in food packaging. Despite these benefits, PLA remains relatively expensive compared to starch and even to other common synthetic polymers such as Polyethylene terephthalate (PET), PP and PS. Additionally, the degradation rate of PLA varies depending on its crystal structure. To address these issues, researchers have sought to develop more affordable and degradable blends of PLA, such as EcoPLA, which incorporates thermoplastic starch (TPS)¹⁷⁻²².

Starch is a versatile polysaccharide derived from cereals like rice, corn and wheat, as well as tubercle roots such as potatoes and cassava. Composed of glucose linked amylose and amylopectin, starch is an environmentally friendly and biodegradable biopolymer that is both abundant and inexpensive. However, its applications have been limited due to its complex macromolecular structure, mechanical brittleness and high water absorption^{19,23,24}. Despite these challenges, blends of starch and other biodegradable polymers have been identified as the most promising way to minimize the limitations of native starches to develop blends of starch and biodegradable polymers to obtain materials with a wide range of application²⁵.

In fact, starch represents the predominant raw material used in biodegradable polymer production, thanks to its low cost. By adding starch to polymeric matrices, the resulting blend might become more degradable, since some microorganisms, such as *Microbacterium aurum*, *Ruminobacter amylophilus* and *Succinimonas amyolytica* utilize starch as a source of nutrients^{26,27}. Furthermore, it can lead to more cost-effective production by reducing the volume fraction of plastic materials used and accumulated after disposal^{17,19,27-29}.

Cotton is one of the most widely used raw materials in the textile industry, second only to polyester in terms of consumption. The main components of cotton fibers are cellulose, hemicellulose, lignin, pectin, protein, ash, fat and wax^{30,31}. The composition of cotton fibers is presented in Table 1. These components undergo constant changes in chemical composition during the cotton growing period. Interestingly, waste cotton from the textile industry and municipal solid waste has similar chemical composition as mature cotton fiber, in which the predominant constituent in both is cellulose, with weight contents that can reach up to 96 wt.%, this cellulose content being higher among natural fibers. Recent studies have shown that the chemical structure of waste cotton contains clusters resembling starch and PLA, which contribute to its biodegradability³⁵⁻³⁸.

In the study conducted by Oliveira et al.¹⁹, the focus was on the eco-efficiency of poly(lactic acid)/starch composites with cotton additions. The authors used a starch content ranging from 0, 3, and 5 wt.% and cotton content ranging from 0, 10,

and 20 wt.%. The results indicated the combination of technical properties (life cycle, environmental impact and ecological footprint) influencing the development of different composite formulations. The authors found that the use of cotton fibers as fillers in these composites resulted in a significantly lower environmental impact in comparison with thermoplastics made exclusively of PLA or PLA/TPS. Additionally, higher proportions of natural cotton fibers were associated with improved overall performance and eco-efficiency.

The use of materials such as PLA and TPS has gained prominence in packaging applications due to their sustainable and biodegradable properties³⁹. PLA possesses barrier properties, making it effective in protecting packaged food and other products from moisture, oxygen and external agents that can compromise their quality^{16,40}. TPS exhibits similar barrier properties as PLA. In some research, TPS-based films are translucent and present good mechanical properties^{41,42}. In addition to these materials, cotton also is an interesting alternative for composites used in packaging⁴³. When added to polymers such as PLA or TPS, cotton can significantly enhance the mechanical and barrier properties of the packaging. This improvement is attributed to the fibrous nature of cotton, which imparts strength, and durability to the composites⁴⁴. The production of cotton, PLA, and TPS composites can be achieved through various methods, such as mechanical blending or extrusion processes. This combination maintains the biodegradability characteristics of the raw materials used⁴⁵. The use of cotton composites in packaging increases the value of by-products from the textile industry, reducing their disposal as garbage^{46,47}.

The novelty of this paper is to propose a biodegradable extruded formulation, using PLA, TPS and cotton fiber, for a biodegradable flexible plastic, with possible use in short shelf-life packaging. A detailed description of the production process of this novel packaging material was provided and its physical, chemical, thermal, mechanical and morphological properties were evaluated. This study contributes to the ongoing efforts to reduce the negative impact of non-biodegradable packaging on the environment and to promote the adoption of eco-friendly alternatives.

2. Experimental Procedures

2.1. Materials

The commercial corn starch (Ingredion Ltda., São Paulo, Brazil) used consisted of 26-30% amylose and 70-74% amylopectin. It contained less than 0.5% gluten and had a moisture content of 12%. The PLA used was purchased from Nature Works, Minnesota, USA, and was of grade 2003D. Its molecular weight was 88,500 Da, and its Mw/Mn was 1.8. The density of the obtained semicrystalline PLA pellet form was 1.24 g/cm³, a value similar to that reported by Solechan et al.⁴⁸ and Farah et al.⁴⁹.

Table 1. Chemical composition of cotton fibers³²⁻³⁴.

Fiber	Cellulose (wt.%)	Lignin (wt.%)	Hemicellulose (wt.%)	Pectin (wt.%)	Wax (wt.%)
Cotton	77 - 96	0.4 - 1.0	3	0.8 - 2.5	0.6

The cotton fiber was donated by AGOPA (Cotton 110 Growers Association, Goiás, Brazil). The fiber has a density of 1.60 g/cm³ a micronaire value of 4.48 and strength of 30.1 MPa. Analytical grade glycerol (15% w/w) was purchased from Vetec Química Fina Ltda (Duque de Caxias, RJ, Brazil).

2.2. Preparation of biodegradable packaging formulations

Prior to extrusion, a mixture of starch and glycerol in 70:30 ratio was manually prepared for the formulation of thermoplastic starch (TPS), according to Albuquerque et al.⁵⁰. This mixture was then processed using a single-screw extruder (AX Plásticos, São Paulo, Brazil), equipped with a single feed and three heating zones, a screw L/D ratio between 30 and 35, in addition to incorporating rolls through which the heated polymer passes to become a film. The temperatures of these zones were maintained at 80, 95, and 115 °C from the feed zone to the die exit³⁷, while the screw speed was set at 30 rpm.

Films with thicknesses ranging from 70 to 100 µm were obtained. Both cotton fibers and TPS were dried in an oven with forced air circulation at 70 °C for about 2 h before processing along with PLA. After drying, the components were manually mixed in the specified proportions, and the resulting cotton incorporated PLA/TPS composites were compounded as per the details presented in Table 2. The experimental procedure is illustrated in Figure 1.

The PLA/TPS/Cotton mixtures were processed using a single-screw extruder, AX Plásticos, São Paulo, Brazil, at temperatures of 160, 170 and 175 °C, with a screw speed of 40 rpm. The extruded films were cut and placed in a metal mold to prepare specimens for the hot compression test. The samples were pressed using an MA098 hot press (Marconi, Piracicaba, Brazil), at a temperature of 90 °C for TPS samples and 170 °C for PLA/TPS/cotton composites for 5 minutes, with a pressure of 6 tons to form the specimens, and then cooled to room temperature in a cold press for 3 minutes.

Table 2. Extruded formulations of cotton incorporated PLA/TPS composites.

Formulations	PLA (wt.%)	TPS (wt.%)	Cotton (wt.%)
TPS	0	100	0
PLA	100	0	0
95/5/0	95	5	0
90/5/5	90	5	5
85/10/5	85	10	5

wt.% - Weight percentage.

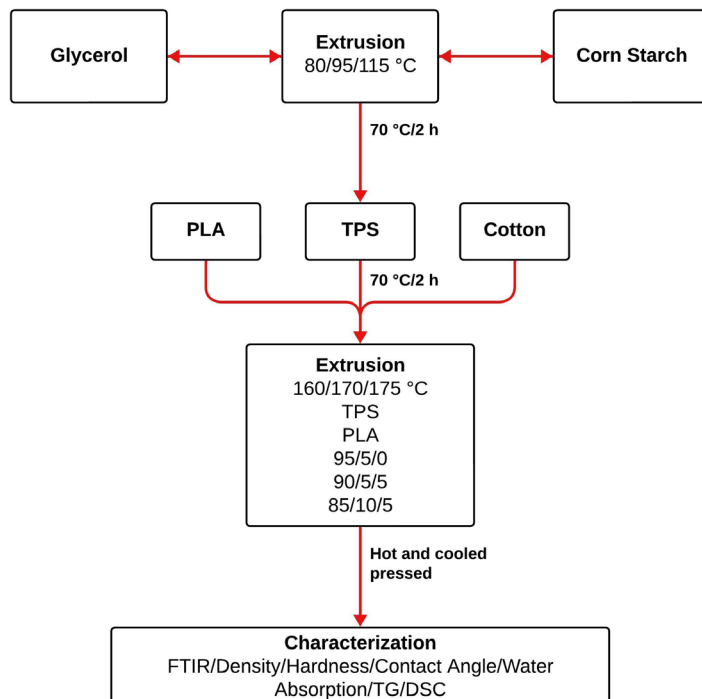


Figure 1. Scheme of the experimental procedure.

2.3. Characterization

2.3.1. Fourier-transform infrared spectroscopy (FTIR)

FTIR analysis was performed using a Nicolet 6700 FTIR spectrometer (Thermo Fisher Scientific). The samples were mounted on an attenuated total reflectance (ATR) accessory equipped with Zinc Selenide (ZnSe) crystal prior to scanning. The spectra were obtained with accumulation of 128 scans and a resolution of 32 cm⁻¹.

2.3.2. Density measurements

The density evaluation was conducted in accordance with the standard procedure outlined in ASTM D792⁵¹. To determine the density, five samples from each group were characterized using a Gehaka DSL910 densimeter (São Paulo, Brazil) at room temperature. The instrument was calibrated before analysis to ensure accuracy and consistency of results. Each group was measured five times, and the mean value was recorded as the final result.

2.3.3. Shore D Hardness

The Shore D hardness tests were conducted in accordance with the ASTM D2240-15 standard⁵². The measurements were taken using a Shore D durometer Type GS 702 (Teclock, Japan). To ensure accuracy, the highest and lowest values obtained from each sample were excluded, and the arithmetic mean of the remaining five determinations was calculated.

2.3.4. Contact angle measurement (CA)

The wettability of the film surface was examined through contact angle measurements using a Ramé-Hart NRLA-100-00 goniometer (Saccasunna, New Jersey, USA). The evolution of the droplet (2 µL) shape was recorded with a CCD camera every 0.2 s for a period of 10 s for each sample, at room temperature. Then, the calculated the arithmetic mean of the 10 measurements was calculated.

2.3.5. Water absorption

The composites water absorption test was conducted following the ASTM D-570 guidelines⁵³. The test involved immersing three samples with dimensions of 20 × 20 × 0.2 mm into a recipient containing distilled water at room temperature over different time periods (2, 24, 48, 72, and 168 h). After the analysis time, excess moisture from the sample was removed, and its mass was measured. The absorption rate was calculated using Equation (1), by determining the difference in weight between the dry and wet samples.

$$\%WA = \frac{W_{final} - W_{initial}}{W_{initial}} \times 100 \quad (1)$$

Where WA is the water absorption, w_{final} is the weight of the composite after water immersion and $w_{initial}$ is the weight of the composite before water immersion.

2.3.6. Thermogravimetric analysis (TGA)

The thermal stability of the extruded samples was evaluated by thermogravimetry (TG/DTG) analysis, using a PerkinElmer STA 6000 (Waltham, Massachusetts, EUA)

simultaneous thermal analyzer with alumina pan, temperature ramp from 30 to 500 °C, heating rate of 10 °C/min and Nitrogen (N₂) atmosphere.

2.3.7. Differential scanning calorimetry (DSC)

The DSC analysis of the extruded samples was performed using a PerkinElmer STA 6000 simultaneous thermal analyzer with alumina pan. The samples were analyzed under N₂ atmosphere, according to the following cycles. First cycle, heating from 30 to 200 °C, at a heating rate of 10 °C/min and maintenance at 200 °C for 2 min. Second cycle, cooling to 30 °C at a cooling rate of 10 °C/min. Third cycle, same temperature range and heating rate of the first cycle (except for the 2 min isothermal). Fourth cycle, conducted at the same temperature range and cooling rate as the second cycle. The data of the second heating curves were considered.

2.3.8. Scanning electron microscopy (SEM)

The surface morphology of the composites was analyzed using scanning electron microscopy (SEM) in a FEI Quanta FEG 250 microscope (Hillsboro, USA), equipped with an Everhart-Thornley secondary electron detector, and operated at an acceleration voltage of 15 kV. The samples were prepared by cutting a square section measuring 20 × 20 mm. Prior to SEM imaging, the samples were coated with gold using a Leica ACE600 (Wetzlar, Germany) sputtering machine to enhance conductivity and image quality.

3. Results and Discussion

3.1. FTIR Results

The aim of the FTIR analysis was to investigate the chemical structure and interactions between cotton, TPS, and PLA in the different formulations. The FTIR spectra are presented in Figure 2.

The FTIR of cotton showed an absorption band between 3500 – 3000 cm⁻¹, related to the hydroxyl group (OH)⁵⁰.

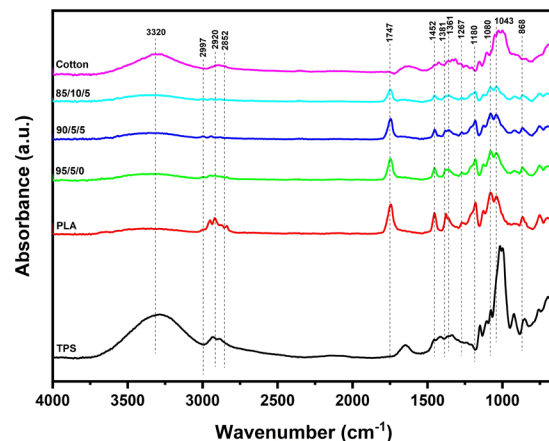


Figure 2. FTIR-ATR spectra of formulations.

The bands at 2915 and 2850 cm^{-1} were assigned to the asymmetric and symmetric CH_2 stretching mode of aliphatic hydrocarbon chains in the cotton wax. Cotton wax is mainly responsible for the hydrophobicity and low water wettability of raw cotton fibers, in addition to protecting the fibers from microbial degradation of underlying carbohydrates, such as cellulose. Previous studies⁵⁴⁻⁵⁸ have assigned a broad band centered at 1620 cm^{-1} to the OH bending mode of adsorbed water. A few bands in the 1500–1200 cm^{-1} region to both CH_2 deformations and C–O–H bending vibrations, and intense bands in the 1200–900 cm^{-1} region are attributed to the stretching modes of C–O and C–C vibrations. The bands from 800 to 700 cm^{-1} represent the contributions from two crystalline forms of cotton cellulose, in which the type of cellulose is associated with the plant's origin and can directly influence the mechanical properties of cotton⁵⁹⁻⁶².

The bands of the TPS occurred between 3600 and 3300 cm^{-1} , corresponding to the stretching of the OH group of the starch, water and glycerol present in TPS. The bands at 2924 and 2893 cm^{-1} are due to the symmetrical or asymmetric stretching of the C–H, H–C–H and C–OH bonds. The band between 1640 and 1600 cm^{-1} is related to the water vibrations present in the TPS, and the band at 856 cm^{-1} corresponds to the conformation of the α D-glucose bonds of starch⁶³⁻⁶⁵.

PLA presented distinctive infrared bands corresponding to its chemical structure: (i) at 868 cm^{-1} , corresponding to the C–C stretching band; (ii) at 1267, 1180, 1128, 1080, and 1043 cm^{-1} , corresponding to the C–O stretching bands; (iii) at 1381 and 1361 cm^{-1} , corresponding to the C–H deformation bands; (iv) at 1452 cm^{-1} , corresponding to the deformation vibration of $-\text{CH}_2$; (v) at 1747 cm^{-1} , corresponding to the C=O stretching of the carbonyl groups; and (vi) at 2997, 2920, 2852, cm^{-1} , corresponding to the C–H stretching bands⁶⁶⁻⁷².

All spectra of the PLA/TPS/cotton composite revealed distinct signals from PLA, TPS, and cotton, confirming

the presence of physical interaction among the formulated compounds. The integration of composite elements through the extrusion process facilitated this interaction, resulting in the emergence of specific bands associated with TPS and cotton within the PLA matrix.

3.2. Density, hardness and contact angle measurement

Table 3 summarizes the results obtained for density, hardness and contact angle of the formulations.

The density results of the composites ranged from 1.06 to 1.32 g/cm^3 , these values of PLA and TPS samples were in agreement with literature data, where in the work of Lohar et al.⁷³ and Salazar-Sánchez et al.⁷⁴, which the density of PLA composites varying in 1.2–1.3 g/cm^3 . Considering the standard deviation, no significant changes in density were observed. It is important to take into consideration that natural fibers as reinforcement in composites cause mechanical obstruction of the polymer molecules, resulting in an increase of volume fraction and reducing density if higher amounts of fibers will be used^{59,75}. The addition of cotton fibers caused a reduction in density, as observed in the result of the 90/5/5 composite, compared to the 95/5/0 composite. However, the addition of 10 wt.% caused an increase in density, as observed in the 85/10/5 group.

As for the hardness values, the incorporation of cotton fibers in the formulations increased the values, making them higher than those of PLA and TPS. Addition of 5 wt.% cotton fibers have been reported to improve the hardness of the composites⁷⁶⁻⁷⁸. The formation of the blend through the mixture of TPS with PLA, along with the addition of cotton fibers, promotes good homogenization, resulting in increased hardness.

The contact angle of PLA (93.06°) presented in Table 2, as well as in Figure 3 was consistent with previously reported values^{79,80}. The addition of TPS and cotton fiber to PLA can lead to a decrease in contact angle.

Table 3. Physical properties of extruded PLA/TPS/Cotton formulations: density, hardness, and contact angle measurements.

Formulations	Density (g/cm^3)	Hardness (Shore D)	Contact Angle (°)
TPS	1.24 ± 0.21	64.00 ± 1.87	18.16 ± 0.33
PLA	1.06 ± 0.21	17.00 ± 0.71	93.06 ± 0.07
95/5/0	1.14 ± 0.08	52.60 ± 1.14	89.77 ± 0.04
90/5/5	1.12 ± 0.24	70.20 ± 2.77	81.84 ± 0.43
85/10/5	1.32 ± 0.19	71.80 ± 2.05	87.00 ± 0.09

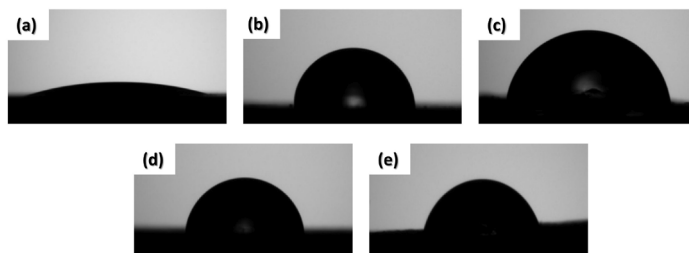


Figure 3. Contact angle between water and processed formulations surface: (a) TPS; (b) PLA; (c) 95/5/0; (d) 90/5/5, and (e) 85/10/5.

As expected, TPS promoting an increase in water absorption, the contact angle decreased by approximately 12% when the PLA/TPS/Cotton proportion was 90/5/5 wt.%, and by approximately 6.5% in the 85/10/5 wt.% formulation, compared to neat PLA. These results suggest a hydrophilic tendency, which can facilitate the biodegradation process of the packaging material at the end of its life cycle, due to the hydrophilic nature of the material, accelerates degradation through the attack of microorganisms, as described in the introduction.

3.3. Water absorption

The water absorption results for PLA/TPS/Cotton composites are presented in Figure 4 and Table 4.

Regarding the absorption of water in the PLA/TPS/Cotton mixtures, the water absorption significantly reduced in comparison with neat TPS. This occurred due to the difference in the chemical structure between PLA and TPS. TPS exhibits highly hydrophilic characteristics due to its preparation process, which may involve the presence of water, starch, glycerol, sorbitol, or glucose. On the other hand, PLA has a hydrophobic nature owing to the presence of highly hydrophobic aliphatic polyesters in its chemical chain. In PLA/TPS/Cotton formulations, the water absorption was lower than 7 wt.% due to the hydrophobic character of the PLA, which was present in higher proportion. In addition, the formulation 85/10/5 showed the maximum value of water absorption (6.291%) after 72 h, which can be attributed to the increased TPS content. The variation in water absorption is directly related to the contact angle results presented in Table 3 and Figure 3. Due to its hydrophilic nature, TPS exhibited significantly higher water absorption values, resulting in lower contact angle values during the measurement. This implies that the addition of TPS in the formulations reduced the contact angle, as observed in the 95/5/0, 90/5/5, and 85/10/5 formulations, which yielded values of 89.77, 81.84, and 87.00, respectively, compared

to the pure PLA value of 93.06. Furthermore, the addition of TPS altered the water absorption values, where pure PLA showed a value of 0.432% after 72 hours of testing, while the 95/5/0, 90/5/5, and 85/10/5 formulations exhibited absorptions of 0.921, 1.011 and 6.291%, respectively.

3.4. Thermal analysis

The thermal decomposition of the TPS, PLA and TPS/PLA/Cotton composites was studied by thermogravimetric analysis (TGA). Figure 5a shows the weight loss vs. temperature curves. Their corresponding first-derivative curves (DTG) are shown in Figure 5b.

Additionally, Table 5 shows some relevant thermal parameters, such as the degradation onset temperature (T_{onset}), the maximum degradation temperature (T_{max}) and residue percentages obtained from the curves. The decomposition profile of TPS is in accordance with data from the literature.

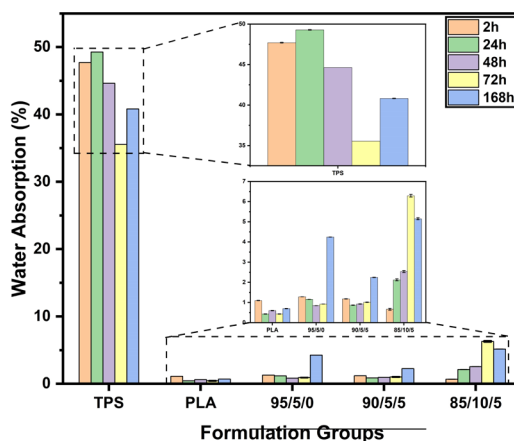


Figure 4. Water absorption results for PLA/TPS/Cotton composites.

Table 4. Water absorption results for PLA/TPS/Cotton composites.

Formulations	Water Absorption (%)				
	2 h	24 h	48 h	72 h	168 h
TPS	47.700 ± 0.017	49.280 ± 0.019	44.630 ± 0.000	35.540 ± 0.000	40.820 ± 0.011
PLA	1.097 ± 0.008	0.432 ± 0.008	0.599 ± 0.008	0.432 ± 0.008	0.699 ± 0.008
95/5/0	1.281 ± 0.001	1.161 ± 0.001	0.841 ± 0.001	0.921 ± 0.001	4.245 ± 0.001
90/5/5	1.179 ± 0.009	0.870 ± 0.009	0.926 ± 0.009	1.011 ± 0.009	2.245 ± 0.009
85/10/5	0.664 ± 0.049	2.120 ± 0.049	2.533 ± 0.050	6.291 ± 0.064	5.150 ± 0.049

Table 5. Summary of TGA and DTG thermal parameters of TPS, PLA and TPS/PLA/Cotton composites.

Formulations	T_{onset} (°C)	T_{max} (°C)	T_{endset} (°C)	Residues (%)
TPS	270.4	309.4	329.1	9.76
PLA	320.6	346.2	364.5	1.95
95/5/0	330.7	359.2	377.5	0.99
90/5/5	295.2	322.9	359.6	2.06
85/10/5	310.8	338.5	364.6	5.87

Stasi et al.⁸¹ reported the occurrence of two main stages⁶⁷. First, the removal of physically adsorbed water followed by evaporation of the glycerol, between 50 and 250 °C. Second, the degradation of the two main components (amylose and amylopectin) of TPS, between 250 and 350 °C, with a final residue of about 9.8%. The decomposition of TPS can be confirmed by analyzing the DTG profile, which exhibited two peaks, indicative of two main mass loss processes. The thermal decomposition profile of PLA agrees with that observed by Palai et al.²⁰, who observed a single mass loss step corresponding to polymer degradation occurred in the range between 97 to 350 °C. However, the DTG profile show two overlapping peaks, which may indicate the presence of additives or might even explain the presence of about 2% of residues in the TG curve of PLA, due to the fact that at this temperature, it is not possible to completely degrade the PLA.

The thermal profiles and data from Table 5 suggest that the presence of TPS increased the thermal stability of PLA, but the presence of cotton tended to decrease this stability. The 95/5/0 formulation showed higher T_{onset} and T_{max} values than PLA, but these temperatures decreased in samples containing cotton (90/5/5 and 85/10/5), this occurred due to the lower thermal stability of cotton fibers, which, when added, reduced the stability of the formulations. Lerma-Canto et al.⁸² observed similar behavior when working with TPS/PLA composites to which hemp oil was added as a plasticizer. The values of

T_{onset} and T_{max} are higher in the 95/5/0 formulation, where the group exhibited values of 330.7 and 359.2 °C, respectively.

Figure 5c exhibits the DSC curves for the second heating of samples. The second curve can reveal information about multiple thermal transitions, such as secondary crystallization, structural changes, or molecular relaxations. It is possible to observe a small endothermic peak at approximately 155 °C for TPS, which is attributed to the melting of crystals that may exist in the structure. Its glass-transition temperature (T_g) occurred at around 88 °C, although it was difficult to observe, as reported by other authors^{79,81}.

From the 85/10/5 formulation, it is possible to observe an increase in thermal stability due to the presence of TPS. This resulted in a melting temperature (T_m) of 153 °C. On the other hand, in the formulation with lower TPS content and the presence of cotton (90/5/5), the peak of melting (T_m) decreased, indicating disruption of the crystalline network.

Overall, the T_g , crystallization temperature (T_c) and T_m showed little variation with the addition of TPS and cotton fibers. The T_g of the formulations ranged from 88 to 98 °C, with the lowest obtained for TPS, while the 85/10/5 formulation exhibited the highest T_g , as highlighted in the blue region of Figure 5c. PLA and the 95/5/0 and 90/5/5 formulations practically showed no significant change in T_g , with PLA having a T_g of 94 °C, and the 95/5/0 and 90/5/5 formulations having a T_g of 95 °C. The T_c in the formulations, highlighted in the green region of Figure 5c, showed minimal variation with the addition of TPS and cotton fibers.

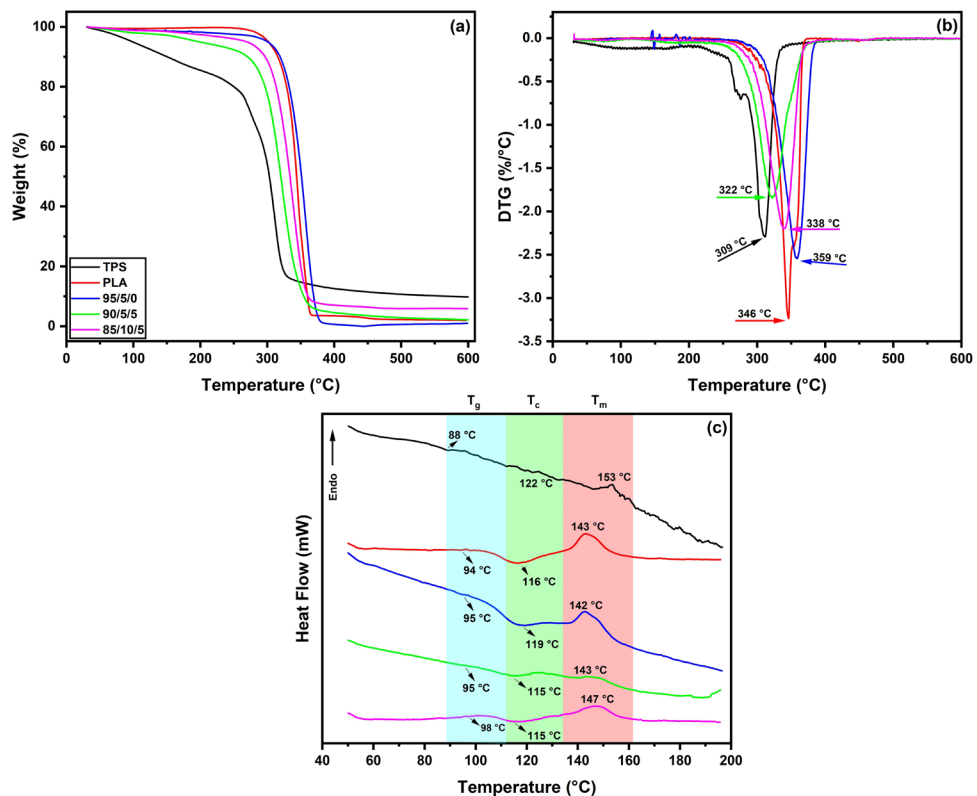


Figure 5. Thermal analysis for TPS, PLA and TPS/PLA/Cotton composites: (a) TGA curves, (b) DTG curves, and (c) DSC curves.

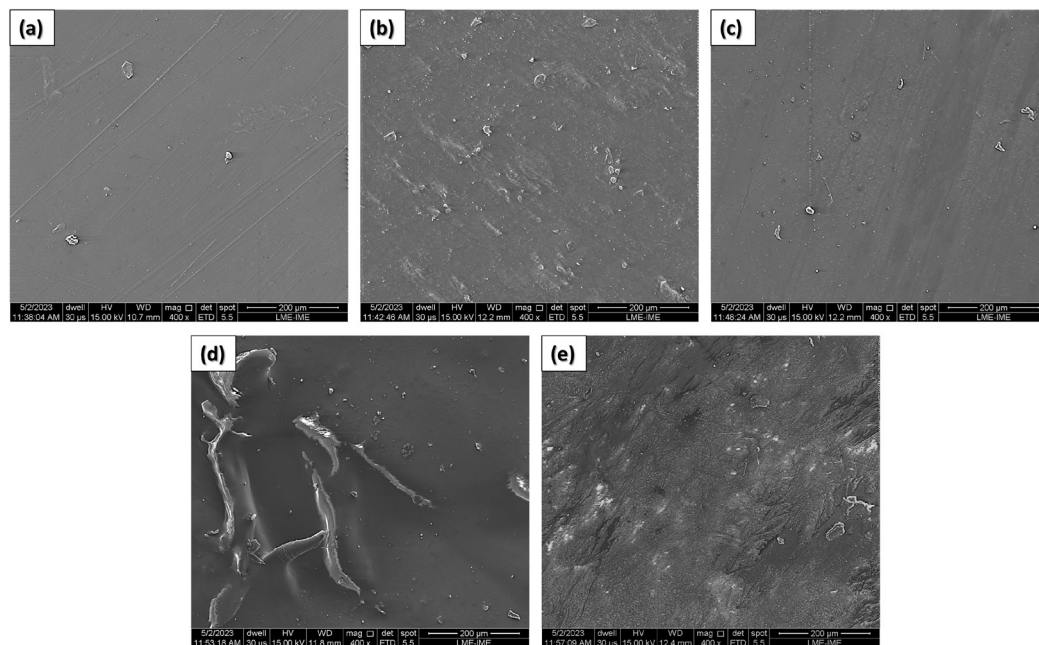


Figure 6. SEM images of the analyzed composite surfaces: (a) PLA; (b) TPS; (c) 95/5/0; (d) 90/5/5, and (e) 85/10/5.

TPS reached the highest T_c value, reaching 122 °C, while for PLA and the PLA/TPS/Cotton composites, T_c ranged from 115 to 119 °C. Regarding the T_m in the formulations, indicated in the red region of Figure 5c, TPS exhibited a T_m of 153 °C, while PLA recorded a T_m of 143 °C. The combination of the two polymers in the 95/5/0 formulation resulted in a slight reduction, presenting a T_m of 142 °C. The inclusion of cotton fibers, forming the 90/5/5 formulation, caused a small increase in T_m , reaching 143 °C. Finally, the 85/10/5 formulation, with a higher TPS content, exhibited a T_m of 147 °C.

3.5. Scanning electron microscopy (SEM)

Figure 6 shows the SEM images of PLA, TPS, and PLA/TPS/Cotton composites. PLA exhibited a smooth surface. It was possible to observe a plasticizing effect of glycerol in the extruded starch, along with some residues of starch granules and a relatively rough surface. An increase in roughness was observed in the PLA/TPS (95/5/0) formulation compared to the PLA matrix. As observed in thermal analysis, glycerol caused a plasticizing effect on PLA macromolecules by increasing polymer chain mobility and decreasing inter-chain interactions. Consequently, a better dispersion of PLA/TPS macromolecules occurred^{65,69}.

The incorporation of TPS and cotton in the PLA matrix promoted surface roughness and the presence of some defects, with protruding cotton fibers dispersed unevenly throughout the matrix. The cotton fibers are embedded within the polymers. This is attributed to the rearrangements between the polymeric chains and the smaller organic glycerol molecules, which interact, allowing for miscibility^{37,64}. Although the hydrophilicity of these mixtures increased compared to pure PLA, this was due to the orientation of the OH groups of the TPS and fiber molecules towards the surface.

4. Conclusions

In this paper, the influence of TPS and cotton fiber on the wetting behavior, morphological, physical, chemical, and thermal properties of PLA, were analyzed. No significant changes in the density were observed, although the presence of cotton fiber slightly increased the hardness results. FTIR analysis revealed a physical interaction between the components. The contact angles of the mixtures with PLA, TPS and cotton decreased slightly compared to neat PLA, with a more pronounced effect in the presence of cotton fiber. TPS exhibited higher water absorption compared to PLA and the formulations, which was attributed to its hydrophilic nature. Comparison of the formulations after 72 h of immersion in water revealed that the 85/10/5 formulation had the maximum water absorption value. DSC analysis indicated that all formulations exhibited a single peak for both crystallization and melting, suggesting good homogeneity and interaction among the components, which was further supported by SEM analysis. The hydrophilic tendency of the composites is expected to contribute to their biodegradation process in the end-of-life cycle of packaging materials. The 85/10/5 formulation exhibited properties that make it particularly well-suited for packaging applications and represents a sustainable alternative to conventional materials.

5. Acknowledgements

We thank the Carlos Chagas Filho Foundation for Research Support of the State of Rio de Janeiro (FAPERJ) and the National Council for Scientific and Technological Development (CNPq) for financial support. This study was financed in part by the Coordination for the Improvement of Higher Education Personnel – Brazil (CAPES) – Funding Code 001.

6. References

- Chen D, Zhang Y, Xu Y, Nie Q, Yang Z, Sheng W, et al. Municipal solid waste incineration residues recycled for typical construction materials: a review. *RSC Adv.* 2022;12(10):6279-91. <http://dx.doi.org/10.1039/D1RA08050D>.
- Wang Q, Chen W, Zhu W, McClements DJ, Liu X, Liu F. A review of multilayer and composite films and coatings for active biodegradable packaging. *NPJ Sci Food.* 2022;6(1):1-16. <http://dx.doi.org/10.1038/s41538-022-00132-8>.
- Davis G, Song JH. Biodegradable packaging based on raw materials from crops and their impact on waste management. *Ind Crops Prod.* 2006;23(2):147-61. <http://dx.doi.org/10.1016/j.indcrop.2005.05.004>.
- Wu J, Sun Q, Huang H, Duan Y, Xiao G, Le T. Enhanced physico-mechanical, barrier and antifungal properties of soy protein isolate film by incorporating both plant-sourced cinnamaldehyde and facile synthesized zinc oxide nanosheets. *Colloids Surf B Biointerfaces.* 2019;180:31-8. <http://dx.doi.org/10.1016/j.colsurfb.2019.04.041>.
- Boussetta A, Benhamou AA, Chari H, Ablouh EH, Mennani M, Kasbaji M, et al. Formulation and characterization of chitin-starch bio-based wood adhesive for the manufacturing of formaldehyde-free composite particleboards. *Waste Biomass Valoriz.* 2023;14(11):3671-87. <http://dx.doi.org/10.1007/s12649-023-02091-x>.
- Tardy BL, Richardson JJ, Greca LG, Guo J, Bras J, Rojas OJ. Advancing bio-based materials for sustainable solutions to food packaging. *Nat Sustain.* 2022;6(4):360-7. <http://dx.doi.org/10.1038/s41893-022-01012-5>.
- Jouyandeh M, Seidi F, Habibzadeh S, Hasanin M, Wiśniewska P, Rabiee N, et al. An overview of green and sustainable polymeric coatings. *Surf Innov.* 2023. In press. <http://dx.doi.org/10.1680/jsuin.23.00043>.
- Silveira PHPM, Santos MCC, Chaves YS, Ribeiro MP, Marchi BZ, Monteiro SN, et al. Characterization of thermo-mechanical and chemical properties of polypropylene/hemp fiber biocomposites: impact of maleic anhydride compatibilizer and fiber content. *Polymers.* 2023;15(15):3271. <http://dx.doi.org/10.3390/polym15153271>.
- Sudheer S, Bandyopadhyay S, Bhat R. Sustainable polysaccharide and protein hydrogel-based packaging materials for food products: a review. *Int J Biol Macromol.* 2023;248:125845. <http://dx.doi.org/10.1016/j.ijbiomac.2023.125845>.
- MacArthur E. Towards the circular economy, economic and business rationale for an accelerated transition. *Cowes: Ellen MacArthur Foundation;* 2013. p. 21-34.
- Casarejos F, Bastos CR, Rufin C, Frota MN. Rethinking packaging production and consumption vis-à-vis circular economy: a case study of compostable cassava starch-based material. *J Clean Prod.* 2018;201:1019-28. <http://dx.doi.org/10.1016/j.jclepro.2018.08.114>.
- Madrid RRM, Mathews PD, Pimenta BV, Mertins O. Biopolymer-lipid hybrid cubosome for delivery of acemannan. *Iocon.* 2023;14(4):56. <http://dx.doi.org/10.3390/IOCN2023-14486>.
- Barbosa HFG, Piva HL, Matsuo FS, Lima SCG, Souza LEB, Osako MK, et al. Hybrid lipid-biopolymer nanocarrier as a strategy for GBM photodynamic therapy (PDT). *Int J Biol Macromol.* 2023;242:124647. <http://dx.doi.org/10.1016/j.ijbiomac.2023.124647>.
- Urena M, Phùng TTT, Gerometta M, Oliveira LS, Chanut J, Domenek S, et al. Potential of polysaccharides for food packaging applications. Part 1/2: an experimental review of the functional properties of polysaccharide coatings. *Food Hydrocoll.* 2023;144:108955. <http://dx.doi.org/10.1016/j.foodhyd.2023.108955>.
- Zhu H, Cheng JH, Han Z, Han Z. Cold plasma enhanced natural edible materials for future food packaging: structure and property of polysaccharides and proteins-based films. *Crit Rev Food Sci Nutr.* 2021;63(20):4450-66. <http://dx.doi.org/10.1080/10408398.2021.2002258>.
- Taib N-AAB, Rahman MR, Huda D, Kuok KK, Hamdan S, Bakri MK, et al. A review on poly lactic acid (PLA) as a biodegradable polymer. *Polym Bull.* 2023;80(2):1179-213. <http://dx.doi.org/10.1007/s00289-022-04160-y>.
- Gautam RB, Kumar S. Development of protein based films with nanoparticle as strengthening material for biodegradable packaging: a review. *Int J Agric Innov Res.* 2017;5:790-805.
- Hu B. Biopolymer-based lightweight materials for packaging applications. In: Yang Y, Xu H, Yu X, editors. *Lightweight materials from biopolymers and biofibers.* Washington, DC: ACS Publications; 2014. p. 239-55. <http://dx.doi.org/10.1021/bk-2014-1175.ch013>.
- Oliveira SA, Nunes de Macedo JR, Rosa DS. Eco-efficiency of poly (lactic acid)-Starch-Cotton composite with high natural cotton fiber content: environmental and functional value. *J Clean Prod.* 2019;217:32-41. <http://dx.doi.org/10.1016/j.jclepro.2019.01.198>.
- Palai B, Biswal M, Mohanty S, Nayak SK. In situ reactive compatibilization of polylactic acid (PLA) and thermoplastic starch (TPS) blends; synthesis and evaluation of extrusion blown films thereof. *Ind Crops Prod.* 2019;141:111748. <http://dx.doi.org/10.1016/j.indcrop.2019.111748>.
- Rahmatbadi D, Ghasemi I, Baniassadi M, Abrinia K, Baghani M. 3D printing of PLA-TPU with different component ratios: fracture toughness, mechanical properties, and morphology. *J Mater Res Technol.* 2022;21:3970-81. <http://dx.doi.org/10.1016/j.jmrt.2022.11.024>.
- Soleyman E, Aberoumand M, Rahmatbadi D, Soltanmohammadi K, Ghasemi I, Baniassadi M, et al. Assessment of controllable shape transformation, potential applications, and tensile shape memory properties of 3D printed PETG. *J Mater Res Technol.* 2022;18:4201-15. <http://dx.doi.org/10.1016/j.jmrt.2022.04.076>.
- Apriyanto A, Compart J, Fettke J. A review of starch, a unique biopolymer—Structure, metabolism and in planta modifications. *Plant Sci.* 2022;318:111223. <http://dx.doi.org/10.1016/j.plantsci.2022.111223>.
- Muthukumar P, Suresh Babu P, Shyamalagowri S, Aravind J, Kamaraj M, Govarthanan M. Polymeric biomolecules based nanomaterials: production strategies and pollutant mitigation as an emerging tool for environmental application. *Chemosphere.* 2022;307:136008. <http://dx.doi.org/10.1016/j.chemosphere.2022.136008>.
- Temesgen S, Rennert M, Tesfaye T, Nase M. Review on spinning of biopolymer fibers from starch. *Polymers.* 2021;13(7):1121. <http://dx.doi.org/10.3390/polym13071121>.
- Valk V, Eeuwema W, Sarian FD, van der Kaaij RM, Dijkhuizen L. Degradation of granular starch by the bacterium *Microbacterium aurum* strain B8: a involves a modular α -amylase enzyme system with FNIII and CBM25 domains. *Appl Environ Microbiol.* 2015;81(19):6610-20. <http://dx.doi.org/10.1128/AEM.01029-15>.
- Hua D, Hendriks WH, Xiong B, Pellikaan WF. Starch and cellulose degradation in the rumen and applications of metagenomics on ruminant microorganisms. *Animals.* 2022;12(21):3020. <http://dx.doi.org/10.3390/ani12213020>.
- Ochoa TA, Almendárez BEG, Reyes AA, Pastrana DMR, López GFG, Bellosso OM, et al. Design and characterization of corn starch edible films including beeswax and natural antimicrobials. *Food Bioprocess Technol.* 2017;10(1):103-14. <http://dx.doi.org/10.1007/s11947-016-1800-4>.
- Alcázar-Alay SC, Meireles MAA. Physicochemical properties, modifications and applications of starches from different botanical sources. *Food Sci Technol.* 2015;35(2):215-36. <http://dx.doi.org/10.1590/1678-457X.6749>.

30. Basiak E, Lenart A, Debeaufort F. Effect of starch type on the physico-chemical properties of edible films. *Int J Biol Macromol.* 2017;98:348-56. <http://dx.doi.org/10.1016/j.ijbiomac.2017.01.122>.
31. Viot CR, Wendel JF. Evolution of the cotton genus, *Gossypium*, and its domestication in the Americas. *Crit Rev Plant Sci.* 2023;42(1):1-33. <http://dx.doi.org/10.1080/07352689.2022.2156061>.
32. Chokshi S, Parmar V, Gohil P, Chaudhary V. Chemical composition and mechanical properties of natural fibers. *J Nat Fibers.* 2022;19(10):3942-53. <http://dx.doi.org/10.1080/15440478.2020.1848738>.
33. Ioelovich M, Leykin A. Structural investigations of various cotton fibers and cotton celluloses. *BioResources.* 2008;3(1):170-7. <http://dx.doi.org/10.15376/biores.3.1.170-177>.
34. Dorez G, Ferry L, Sonnier R, Taguet A, Lopez-Cuesta JM. Effect of cellulose, hemicellulose and lignin contents on pyrolysis 1271 and combustion of natural fibers. *J Anal Appl Pyrolysis.* 2014;107:323-31. <http://dx.doi.org/10.1016/j.jaap.2014.03.017>.
35. Jawaid M, Abdul Khalil HPS. Cellulosic/synthetic fibre reinforced polymer hybrid composites: a review. *Carbohydr Polym.* 2011;86(1):1-18. <http://dx.doi.org/10.1016/j.carbpol.2011.04.043>.
36. Yan L, Kasal B, Huang L. A review of recent research on the use of cellulosic fibres, their fibre fabric reinforced cementitious, geo-polymer and polymer composites in civil engineering. *Compos, Part B Eng.* 2016;92:94-132. <http://dx.doi.org/10.1016/j.compositesb.2016.02.002>.
37. Lu L, Fan W, Meng X, Xue L, Ge S, Wang C, et al. Current recycling strategies and high-value utilization of waste cotton. *Sci Total Environ.* 2023;856:158798. <http://dx.doi.org/10.1016/j.scitotenv.2022.158798>.
38. Huang W, Wu F, Han W, Li Q, Han Y, Wang G, et al. Carbon footprint of cotton production in China: Composition, spatiotemporal changes and driving factors. *Sci Total Environ.* 2022;821:153407. <http://dx.doi.org/10.1016/j.scitotenv.2022.153407>.
39. Li X, Lin Y, Liu M, Meng L, Li C. A review of research and application of polylactic acid composites. *J Appl Polym Sci.* 2023;140(7):e53477. <http://dx.doi.org/10.1002/app.53477>.
40. Swetha TA, Ananthi V, Bora A, Sengottuvelan N, Ponnuchamy K, Muthusamy G, et al. A review on biodegradable polylactic acid (PLA) production from fermentative food waste: its applications and degradation. *Int J Biol Macromol.* 2023;234:123703. <http://dx.doi.org/10.1016/j.ijbiomac.2023.123703>.
41. Zhao X, Wang Y, Chen X, Yu X, Li W, Zhang S, et al. Sustainable bioplastics derived from renewable natural resources for food packaging. *Matter.* 2023;6(1):97-127. <http://dx.doi.org/10.1016/j.matt.2022.11.006>.
42. Soulestin J, Prashantha K, Lacrampe MF, Krawczak P. Bioplastics based nanocomposites for packaging applications. In: Pilla S, editor. *Handbook of bioplastics and biocomposites engineering applications.* Hoboken: John Wiley & Sons; 2011. p. 76-119. <http://dx.doi.org/10.1002/9781118203699.ch4>.
43. Vadivu SK. Mechanical characterization of coir fiber and cotton fiber reinforced unsaturated polyester composites for packaging applications. *Journal of Applied Packaging Research.* 2017;9(2):2.
44. Lindström T, Österberg F. Evolution of biobased and nanotechnology packaging: a review. *Nord Pulp Paper Res J.* 2020;35(4):491-515. <http://dx.doi.org/10.1515/npprj-2020-0042>.
45. Martinez Villadiego K, Arias Tapia MJ, Useche J, Escobar Macias D. Thermoplastic starch (TPS)/polylactic acid (PLA) blending methodologies: a review. *J Polym Environ.* 2022;30(1):75-91. <http://dx.doi.org/10.1007/s10924-021-02207-1>.
46. Meekum U, Kingchang P. Compounding oil palm empty fruit bunch/cotton fiber hybrid reinforced poly(lactic acid) biocomposites aiming for high-temperature packaging applications. *BioResources.* 2017;12(3). <http://dx.doi.org/10.15376/biores.12.3.4670-4689>.
47. Radoor S, Karayil J, Shivanna JM, Jayakumar A, Parameswaranpillai J, Siengchin S. Cotton fibers, their composites and applications. In: Rangappa SM, Parameswaranpillai J, Siengchin S, Ozbakkaloglu T, Wang H, editors. *Plant fibers, their composites, and applications.* Cambridge: Elsevier; 2022. p. 379-90. <http://dx.doi.org/10.1016/B978-0-12-824528-6.00003-5>.
48. Solechan S, Suprihanto A, Widyanto SA, Triyono J, Fitriyana DF, Siregar JP, et al. Characterization of PLA/PCL/nano-hydroxyapatite (nHA) biocomposites prepared via cold isostatic pressing. *Polymers.* 2023;15(3):559. <http://dx.doi.org/10.3390/polym15030559>.
49. Farah S, Anderson DG, Langer R. Physical and mechanical properties of PLA, and their functions in widespread applications: a comprehensive review. *Adv Drug Deliv Rev.* 2016;107:367-92. <http://dx.doi.org/10.1016/j.addr.2016.06.012>.
50. Albuquerque MF, Bastos D, Tãlu Ş, Matos R, Pires M, Salerno M, et al. Vapor barrier properties of cold plasma treated corn starch films. *Coatings.* 2022;12(7):1006. <http://dx.doi.org/10.3390/coatings12071006>.
51. ASTM: American Society for Testing and Materials. ASTM D792: standard test methods for density and specific gravity (relative density) of plastics by displacement. West Conshohocken: ASTM; 2020.
52. ASTM: American Society for Testing and Materials. ASTM D2240-15: standard test method for rubber property-durometer hardness. West Conshohocken: ASTM; 2021.
53. ASTM: American Society for Testing and Materials. ASTM D570-25: standard test method for water absorption of plastics. West Conshohocken: ASTM; 2022.
54. Abidi N, Cabrales L, Hequet E. Fourier transform infrared spectroscopic approach to the study of the secondary cell wall development in cotton fiber. *Cellulose.* 2010;17(2):309-20. <http://dx.doi.org/10.1007/s10570-009-9366-1>.
55. Abidi N, Cabrales L, Haigler CH. Changes in the cell wall and cellulose content of developing cotton fibers investigated by FTIR spectroscopy. *Carbohydr Polym.* 2014;100:9-16. <http://dx.doi.org/10.1016/j.carbpol.2013.01.074>.
56. Abidi N, Hequet E, Cabrales L, Gannaway J, Wilkins T, Wells LW. Evaluating cell wall structure and composition of developing cotton fibers using Fourier transform infrared spectroscopy and thermogravimetric analysis. *J Appl Polym Sci.* 2008;107(1):476-86. <http://dx.doi.org/10.1002/app.27100>.
57. Liu Y, Thibodeaux D, Gamble G. Development of Fourier transform infrared spectroscopy in direct, non-destructive, and rapid determination of cotton fiber maturity. *Text Res J.* 2011;81(15):1559-67. <http://dx.doi.org/10.1177/0040517511410107>.
58. Liu Y, Kim H-J. Use of Attenuated Total Reflection Fourier Transform Infrared (ATR FT-IR) Spectroscopy in direct, nondestructive, and rapid assessment of developmental cotton fibers grown in planta and in culture. *Appl Spectrosc.* 2015;69(8):1004-10. <http://dx.doi.org/10.1366/15-07876>.
59. Fernandes RAP, da Silveira PHPM, Bastos BC, da Costa Pereira PS, de Melo VA, Monteiro SN, et al. Bio-based composites for light automotive parts: statistical analysis of mechanical properties: effect of matrix and alkali treatment in sisal fibers. *Polymers.* 2022;14(17):3566. <http://dx.doi.org/10.3390/polym14173566>.
60. Chaves YS, da Silveira PHPM, Neuba LM, Junio RFP, Ribeiro MP, Monteiro SN, et al. Evaluation of the density, mechanical, thermal and chemical properties of babassu fibers (*Attalea speciosa*) for potential composite reinforcement. *J Mater Res Technol.* 2023;23:2089-100. <http://dx.doi.org/10.1016/j.jmrt.2023.01.100>.
61. Silveira PHPM, Ribeiro MP, Silva TT, Lima AM, Lemos MF, Oliveira AGBAM, et al. Effect of alkaline treatment and graphene oxide coating on thermal and chemical properties of hemp (*Cannabis sativa* L.) fibers. *J Nat Fibers.* 2022;19(15):12168-81. <http://dx.doi.org/10.1080/15440478.2022.2053265>.

62. Liu Y, Kim H-J. Separation of underdeveloped from developed cotton fibers by attenuated total reflection Fourier transform infrared spectroscopy. *Microchem J.* 2020;158:105152. <http://dx.doi.org/10.1016/j.microc.2020.105152>.
63. Dufresne A. Nanocellulose: from nature to high performance tailored materials. Berlin: De Gruyter; 2012. <http://dx.doi.org/10.1515/9783110254600>.
64. Reiniati I, Hrymak AN, Margaritis A. Recent developments in the production and applications of bacterial cellulose fibers and nanocrystals. *Crit Rev Biotechnol.* 2017;37(4):510-24. <http://dx.doi.org/10.1080/07388551.2016.1189871>.
65. Campano C, Miranda R, Merayo N, Negro C, Blanco A. Direct production of cellulose nanocrystals from old newspapers and recycled newsprint. *Carbohydr Polym.* 2017;173:489-96. <http://dx.doi.org/10.1016/j.carbpol.2017.05.073>.
66. Alfaro MEC, Stares SL, Barra GMO, Hotza D. Effects of accelerated weathering on properties of 3D-printed PLA scaffolds. *Mater Today Commun.* 2022;33:104821. <http://dx.doi.org/10.1016/j.mtcomm.2022.104821>.
67. Varsavas SD, Kaynak C. Weathering degradation performance of PLA and its glass fiber reinforced composite. *Mater Today Commun.* 2018;15:344-53. <http://dx.doi.org/10.1016/j.mtcomm.2017.11.008>.
68. Martín del Campo AS, Robledo-Ortiz JR, Arellano M, Rabelero M, Pérez-Fonseca AA. Accelerated weathering of poly(lactic acid)/agave fiber biocomposites and the effect of fiber-matrix adhesion. *J Polym Environ.* 2021;29(3):937-47. <http://dx.doi.org/10.1007/s10924-020-01936-z>.
69. Lv S, Liu X, Gu J, Jiang Y, Tan H, Zhang Y. Effect of glycerol introduced into PLA based composites on the UV weathering behavior. *Constr Build Mater.* 2017;144:525-31. <http://dx.doi.org/10.1016/j.conbuildmat.2017.03.209>.
70. Lizárraga-Laborín LL, Quiroz-Castillo JM, Encinas-Encinas JC, Castillo-Ortega MM, Burrueal-Ibarra SE, Romero-García J, et al. Accelerated weathering study of extruded polyethylene/poly(lactic acid)/chitosan films. *Polym Degrad Stabil.* 2018;155:43-51. <http://dx.doi.org/10.1016/j.polymdegradstab.2018.06.007>.
71. Copinet A, Bertrand C, Govindin S, Coma V, Couturier Y. Effects of ultraviolet light (315 nm), temperature and relative humidity on the degradation of poly(lactic acid) plastic films. *Chemosphere.* 2004;55(5):763-73. <http://dx.doi.org/10.1016/j.chemosphere.2003.11.038>.
72. Isadounene S, Hammiche D, Boukerrou A, Rodrigue D, Djidjelli H. Accelerated ageing of alkali treated olive husk flour reinforced Poly(lactic acid) (PLA) biocomposites: physico-mechanical properties. *Polym Polymer Compos.* 2018;26(3):223-32. <http://dx.doi.org/10.1177/096739111802600302>.
73. Lohar DV, Nikalje AM, Damle PG. Synthesis and characterization of PLA hybrid composites using bio waste fillers. *Mater Today Proc.* 2023;72:2155-62. <http://dx.doi.org/10.1016/j.matpr.2022.08.276>.
74. Salazar-Sánchez MR, Immirzi B, Solanilla-Duque JF, Zannini D, Malinconico M, Santagata G. *Uromoides dermestoides* Coleopteran action on Thermoplastic Starch/Poly(lactic acid) films biodegradation: a novel, challenging and sustainable approach for a fast mineralization process. *Carbohydr Polym.* 2022;279:118989. <http://dx.doi.org/10.1016/j.carbpol.2021.118989>.
75. Meliande NM, Oliveira MS, Silveira PHPM, Dias RR, Marçal RLSB, Monteiro SN, et al. Curaua-aramid hybrid laminated composites for impact applications: flexural, charpy impact and elastic properties. *Polymers.* 2022;14(18):3749. <http://dx.doi.org/10.3390/polym14183749>.
76. Deka BK, Maji TK. Effect of coupling agent and nanoclay on properties of HDPE, LDPE, PP, PVC blend and *Phargamites karka* nanocomposite. *Compos Sci Technol.* 2010;70(12):1755-61. <http://dx.doi.org/10.1016/j.compscitech.2010.07.010>.
77. Inai NH, Lewandowska AE, Ghita OR, Eichhorn SJ. Interfaces in polyethylene oxide modified cellulose nanocrystal - polyethylene matrix composites. *Compos Sci Technol.* 2018;154:128-35. <http://dx.doi.org/10.1016/j.compscitech.2017.11.009>.
78. Mohan Bhasney S, Mondal K, Kumar A, Katiyar V. Effect of microcrystalline cellulose [MCC] fibres on the morphological and crystalline behaviour of high density polyethylene [HDPE]/poly(lactic acid) [PLA] blends. *Compos Sci Technol.* 2020;187:107941. <http://dx.doi.org/10.1016/j.compscitech.2019.107941>.
79. Calambás Pulgarín HL, Caicedo C, López EF. Effect of surfactant content on rheological, thermal, morphological and surface properties of thermoplastic starch (TPS) and poly(lactic acid) (PLA) blends. *Heliyon.* 2022;8(10):e10833. <http://dx.doi.org/10.1016/j.heliyon.2022.e10833>.
80. Turco R, Ortega-Toro R, Tesser R, Mallardo S, Collazo-Bigliardi S, Chiralt Boix A, et al. Poly(lactic acid)/thermoplastic starch films: effect of cardoon seed epoxidized oil on their chemico-physical, mechanical, and barrier properties. *Coatings.* 2019;9(9):574. <http://dx.doi.org/10.3390/coatings9090574>.
81. Stasi E, Giuri A, Ferrari F, Armenise V, Colella S, Listorti A, et al. Biodegradable carbon-based ashes/maize starch composite films for agricultural applications. *Polymers.* 2020;12(3):524. <http://dx.doi.org/10.3390/polym12030524>.
82. Lerma-Canto A, Gomez-Caturla J, Herrero-Herrero M, Garcia-Garcia D, Fombuena V. Development of poly(lactic acid) thermoplastic starch formulations using maleinized hemp oil as biobased plasticizer. *Polymers.* 2021;13(9):1392. <http://dx.doi.org/10.3390/polym13091392>.